

UniTrans: A Unified Vertical Federated Knowledge Transfer Framework for Enhancing Cross-Hospital Collaboration

Chung-ju Huang, Yuanpeng He, Xiao Han, Wenpin Jiao, Zhi Jin, *Fellow, IEEE*, and Leye Wang, *Member, IEEE*

arXiv:2501.11388v1 [cs.LG] 20 Jan 2025

Abstract—Cross-hospital collaboration has the potential to address disparities in medical resources across different regions. However, strict privacy regulations prohibit the direct sharing of sensitive patient information between hospitals. Vertical federated learning (VFL) offers a novel privacy-preserving machine learning paradigm that maximizes data utility across multiple hospitals. Traditional VFL methods, however, primarily benefit patients with overlapping data, leaving vulnerable non-overlapping patients without guaranteed improvements in medical prediction services. While some knowledge transfer techniques can enhance the prediction performance for non-overlapping patients, they fall short in addressing scenarios where overlapping and non-overlapping patients belong to different domains, resulting in challenges such as feature heterogeneity and label heterogeneity. To address these issues, we propose a novel unified vertical federated knowledge transfer framework (Unitrans). Our framework consists of three key steps. First, we extract the federated representation of overlapping patients by employing an effective vertical federated representation learning method to model multi-party joint features online. Next, each hospital learns a local knowledge transfer module offline, enabling the transfer of knowledge from the federated representation of overlapping patients to the enriched representation of local non-overlapping patients in a domain-adaptive manner. Finally, hospitals utilize these enriched local representations to enhance performance across various downstream medical prediction tasks. Experiments on real-world medical datasets validate the framework’s dual effectiveness in both intra-domain and cross-domain knowledge transfer. The code of UniTrans is available at <https://github.com/Chung-ju/Unitrans>.

Index Terms—Vertical federated learning, knowledge transfer, cross-domain learning.

I. INTRODUCTION

FEDERATED Learning (FL) [1] is a distributed machine learning paradigm that has garnered significant attention for its ability to facilitate collaborative model training while preserving data privacy. In FL, multiple parties independently train models on their local data, sharing only model parameters with a central server that aggregates them into a global model. This global model typically achieves better performance than the individual local models. Unlike centralized machine learning, FL ensures that the raw data from each party remains

private and is not exchanged. FL has been widely adopted by major technology companies, such as Google and Apple, where it is used to enhance services like Face ID, Siri, and predictive text in Gboard [2].

In general, FL can be categorized into two types: Horizontal FL (HFL) and Vertical FL (VFL). HFL was first proposed by Google in their seminal work [1] and is applicable to scenarios where different parties have data with similar feature spaces but different user spaces. The clients in HFL are usually various terminal devices. Each client first trains a local model using isolated data and then sends the model parameters to the server. The server aggregates the model parameters using methods such as FedAvg [1] and then sends the global model back to each client. In contrast, VFL operates in situations where different parties, often organizations, hold distinct feature spaces of the same set of users. The stringent data privacy requirements imposed by regulations such as the Health Insurance Portability and Accountability Act (HIPAA) [3] and the EU’s General Data Protection Regulation (GDPR) [4] have significantly constrained multi-institutional research. In this context, VFL has emerged as a pivotal technology for enabling secure and effective cross-party medical collaboration [5], [6]. Therefore, we take hospital collaboration as scenario, as illustrated in Fig. 1. The VFL task initiator who holds the labels is referred to as the task party \mathcal{P}_t . The data party \mathcal{P}_d , who provide abundant data and collaborate in training/inference, supports the task party. \mathcal{P}_t aims to collaborate with \mathcal{P}_d to provide enhanced healthcare prediction services for overlapping patients.

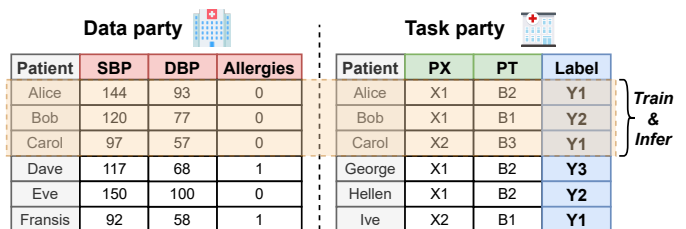


Fig. 1. Healthcare application scenario of VFL.

Motivation. The successful adoption of current VFL methods is highly dependent on how many overlapping samples exist between parties. Hence, most VFL collaborations are conducted by involving at least one giant \mathcal{P}_d with abundant data. For instance, FDN (federated data network) [7] includes anonymous data from one of the largest social network service

Chung-ju Huang, Yuanpeng He, Wenpin Jiao, Zhi Jin, and Leye Wang are with the Key Lab of High Confidence Software Technologies, Ministry of Education, Beijing 100816, China, and also with the School of Computer Science, Peking University, Beijing 100871, China (e-mail: chongruhuang.pku@gmail.com; heyuanpeng@stu.pku.edu.cn; jwp@pku.edu.cn; zhijin@pku.edu.cn; leyewang@pku.edu.cn).

Xiao Han is with School of Economics and Management, Beihang University, Beijing 100191, China (e-mail: xh_bh@buaa.edu.cn).

Manuscript received April 19, 2005; revised August 26, 2015.

providers in China and thus can cover most user samples from other data holders (e.g., customers of banks). However, this makes giant data holders occupy a dominant position over other small data holders in VFL, which could lead to unfair trades and data monopoly in the digital economy.¹ In the scenario depicted in Fig. 1, \mathcal{P}_t is typically a small hospital in remote area, while \mathcal{P}_d is a large hospital with abundant features. The application of VFL by \mathcal{P}_t and \mathcal{P}_d for disease prediction on overlapping patients raises two issues: ① The characteristics and attributes of the data from \mathcal{P}_t are often overshadowed by large \mathcal{P}_d with more extensive features. This dominance hampers the \mathcal{P}_t 's ability to leverage the specificity of local data to provide more personalized treatment for patients. ② Patients need to visit multiple hospitals to access better federated services. However, patients restricted to remote hospitals due to geographical or socioeconomic factors may face unequal access to medical resources. Thus, it is essential to focus on and protect this vulnerable group. To alleviate this defect and expand the application scenarios of VFL, a VFL-based collaborative framework that can benefit local non-overlapping samples is urgently needed.

Status Quo and Challenges. With the advancement of VFL, there has been a growing body of work focusing on the usability of non-overlapping samples [5], [8], [9], [10], [11]. Their common approach involves training on cross-party overlapping samples and transferring federated knowledge to their local non-overlapping samples. However, in real scenarios, especially in healthcare, knowledge transfer is not simplistic. Because non-overlapping patients and overlapping patients may come from different domains, such as from different departments of \mathcal{P}_t . This will lead to two key challenges [12], [13]: feature heterogeneity and label heterogeneity.

- *Feature heterogeneity* [14], [15], [16]. The overlap between \mathcal{P}_t and \mathcal{P}_d may mainly involve patient data from internal medicine departments, which usually include patients with chronic diseases (such as hypertension, diabetes, etc.) [17]. However, non-overlapping patients may come from patient data in surgical departments, involving diseases that require surgical intervention (such as tumors, trauma, etc.) as well as pre- and postoperative evaluations, anesthesia information, postoperative recovery, and other related data.
- *Label heterogeneity* [18], [19], [20], [21]. The label definitions for internal medicine and surgery may be different, resulting in deviations in the model's understanding and use of predicted labels after knowledge transfer [22]. Internal medicine labels may be long-term labels about disease management, such as "well-controlled hypertension", "long-term stable diabetes", etc. Surgical labels might be about surgical risk, acute changes in medical condition, or trauma management, such as "high-risk surgery", "good postoperative recovery", or "acute heart failure" [23].

These challenges are illustrated in Fig. 2. Although the medical and surgical patient populations differ in disease types

and treatments, they often share some underlying physiological characteristics and clinical indicators, which may be highly predictive in tasks such as diagnosis and risk assessment [24], [25]. By transferring knowledge from overlapping patients' data from internal medicine, surgical models can be helped to capture these invariant features, thereby improving the predictive accuracy of non-overlapping patients. If the model learns how to identify the association between hypertension and other complications in internal medicine, and transfers this knowledge to surgery, the model will be able to better predict surgical risks or postoperative complications in surgical patients. We have summarized and compared existing knowledge transfer techniques in Tbl. I (details in Sec II-A), revealing that current approaches are insufficient to simultaneously address both challenges. Therefore, there is an urgent need to develop advanced vertical federated knowledge transfer technologies that can effectively handle both intra-domain and cross-domain scenarios, addressing the challenges posed by complex real-world medical tasks.

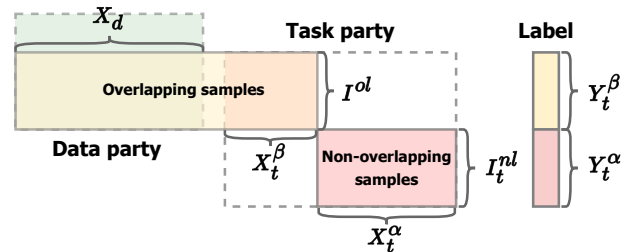


Fig. 2. Two challenges in VFL knowledge transfer.

Our work. We propose a unified framework for vertical federated knowledge transfer (UniTrans) that enables the transfer of medical knowledge from overlapping samples across collaborative healthcare networks to each hospital's local, non-overlapping samples. The key challenge is addressing the issue of feature and label heterogeneity during knowledge transfer. Specifically, overlapping and non-overlapping samples may originate from different domains, requiring effective methods to handle these discrepancies. We begin by employing novel unsupervised federated representation extraction techniques, such as federated singular vector decomposition (FedSVD) [26], to derive federated latent representations from overlapping samples. Next, we introduce a cross-attention-based local knowledge transfer module, designed to effectively distill knowledge from these multi-party federated latent representations into local non-overlapping samples. To enhance knowledge transfer, we incorporate cross-domain adaptation by maximizing the mutual information between the source and target domains, which ensures effective alignment of features across domains. To minimize redundancy in knowledge transfer during multi-party collaboration (involving more than two parties), we incorporate the concept of contrastive learning. This approach enhances the uniqueness of the knowledge acquired through one-to-one learning, ensuring more efficient and targeted knowledge transfer. Finally, each participating hospital can leverage the joint representation of overlapping samples as a guide to enrich the feature representations of its

¹<https://www.theguardian.com/technology/2015/apr/19/google-dominates-search-real-problem-monopoly-data>

local samples through the trained knowledge transfer module. Our proposed knowledge transfer mechanism offers several key advantages:

- *Knowledge transfer to local samples.* Unlike most VFL methods that focus solely on overlapping samples, our proposed mechanism is designed to enhance the prediction performance of local non-overlapping samples across different parties through vertical knowledge transfer. This approach enables hospitals with a limited number of overlapping samples to derive substantial benefits from collaboration, ensuring effective collaboration even in scenarios with sparse overlapping data.
- *Domain-adaptive transfer.* The feature alignment techniques and task-independent transfer mechanisms integrated into UniTrans ensure strong performance in both intra-domain and cross-domain knowledge transfer scenarios. This capability not only enhances the adaptability of the model but also broadens its applicability to diverse real-world scenarios, where feature heterogeneity and label heterogeneity are common challenges.
- *Scalable to multiple hospitals.* Our mechanism achieves efficient multi-party learning with computational complexity that scales linearly with the number of participating hospitals. Simultaneously, it guarantees effective knowledge transfer during multi-party collaboration, leading to enhanced prediction performance.

Contribution. In summary, this work makes the following contributions:

- 1) To the best of our knowledge, this work is the first one to explore how to enable vertical knowledge transfer from overlapping samples to each hospital’s non-overlapping samples in a domain-adaptive manner.
- 2) We propose a novel domain-adaptive vertical-knowledge-transfer framework, UniTrans, to transfer medical knowledge from overlapping samples to local samples. UniTrans demonstrates a dual capability in knowledge transfer, making it highly versatile and impactful in both intra-domain and cross-domain applications.
- 3) Experiments conducted on seven real-world medical datasets validate the effectiveness of our mechanism for knowledge transfer and the generalizability of the enriched feature representations for local samples. These results highlight how UniTrans empowers hospitals with limited medical resources to deliver improved healthcare services through VFL collaboration.

II. RELATED WORK

A. Vertical Knowledge Transfer

Existing VFL mechanisms [27], [28], [29] primarily focus on improving the prediction performance of overlapping samples. In contrast, this work focuses on transferring knowledge from overlapping samples to enhance the prediction performance of each party’s local non-overlapping samples.

We summarize the prior knowledge transfer techniques in Tbl. I. FTL trains feature extractors for \mathcal{P}_t and \mathcal{P}_d on overlapping samples, mapping heterogeneous feature spaces to

a common latent subspace [11]. FTL relies on source domain labels during training. Therefore, while FTL can address feature heterogeneity, it cannot handle label heterogeneity. VFL-Infer [8] transfers knowledge from the federated model on overlapping samples to local models by extracting soft labels generated by the federated model. FedCVT [9] utilizes existing representations to estimate the missing feature representations for \mathcal{P}_t and predicts pseudo-labels for unlabeled samples to construct an extended training set. Both VFL-Infer and FedCVT are incapable of handling scenarios with both feature and label heterogeneity. VFedTrans [5] first uses FedSVD [26] on overlapping samples to obtain federated latent representations, and then trains a single auto-encoder on overlapping and non-overlapping samples to perform representation distillation. This makes VFedTrans unable to handle the feature heterogeneity problem of overlapping and non-overlapping samples. In the knowledge transfer of VFedTrans, only overlapping samples can obtain the distillation loss constraint of the federated latent representation. This further reduces the effectiveness of knowledge transfer for non-overlapping samples. FedHSSL [10] first uses cross-party self-supervised learning (SSL) to train a cross-party encoder on overlapping samples, and then uses the cross-party encoder to train a local encoder on local samples (including overlapping and non-overlapping). Although VFedTrans and FedHSSL can address label heterogeneity, they still fail to resolve feature heterogeneity. Overall, existing vertical knowledge transfer techniques are unable to simultaneously address feature heterogeneity and label heterogeneity. The proposed UniTrans overcomes this limitation, enabling the improvement of prediction performance for non-overlapping samples in more complex scenarios.

TABLE I
COMPARISON OF EXISTING KNOWLEDGE TRANSFER TECHNIQUES IN VFL.

†Method	Feature Heterogeneity	Label Heterogeneity
VFL-Infer [8]	No	No
FedCVT [9]	No	No
FedHSSL [10]	No	Yes
VFedTrans [5]	No	Yes
FTL [11]	Yes	No
Ours	Yes	Yes

B. Federated Domain Learning

Existing federated domain learning [30], [31], [32] primarily focuses on improving the prediction performance of the target domain in HFL scenarios. Only a small number of studies [33], [34] have focused on the domain learning problem in VFL. PrADA [33] proposes a vertical federated adversarial domain adaptation method aimed at learning high-order features for multiple domains on overlapping samples across multiple participants, thereby improving the interpretability of predictions. Fed-CRFD [34] investigates domain shift issues caused by different modalities on overlapping samples to facilitate MRI reconstruction. These studies focus solely on domain learning on overlapping samples. In contrast, our work aims to address the cross-domain challenges in knowledge transfer from overlapping to non-overlapping samples.

III. PROBLEM FORMULATION

In this section, we clarify the definitions of key concepts used in this paper. Afterward, we formulate our research problem. The used notations can be found in Appendix.

A. Concepts

Our approach enables non-overlapping patients from all hospitals to benefit from the collaboration. VFL typically involves a two-party scenario [35], consisting of one task hospital \mathcal{P}_t and one data hospital \mathcal{P}_d .

- *Task Hospital.* A task hospital \mathcal{P}_t has a set of patients with features X_t and a task label Y_t to predict. The patient IDs of \mathcal{P}_t are denoted as I_t .
- *Data Hospital.* A data hospital \mathcal{P}_d has a set of samples with features X_d . The data hospital's sample IDs are denoted as I_d .

Patient IDs overlapping between \mathcal{P}_t and \mathcal{P}_d are referred to as $I_t^{ol} = I_d^{ol} = I_t \cap I_d$, while non-overlapping IDs of \mathcal{P}_t are referred to as $I_t^{nl} = I_t \setminus I_t^{ol}$.

B. Research Problem

Given a task hospital \mathcal{P}_t and a data hospital \mathcal{P}_d , holding overlapping patient data $H_t^{ol} \in \mathbb{R}^{I_t^{ol} \times X_t^\beta}$ and $H_d^{ol} \in \mathbb{R}^{I_d^{ol} \times X_d}$ respectively. \mathcal{P}_t also holds the target non-overlapping patient data $H_t^{nl} \in \mathbb{R}^{I_t^{nl} \times X_t^\alpha}$. The feature domains X_t^β and X_t^α and the label domains Y_t^{nl} and Y_t^{ol} may be heterogeneous. The objective is to design a knowledge transfer mechanism to predict the task label Y_t^{nl} of \mathcal{P}_t 's non-overlapping patients data H_t^{nl} as accurately as possible.

Remark. Traditional VFL frameworks often require that $I_t = I_d$. However, our vertical federated knowledge transfer setting only needs that $I_t^{ol} \neq \emptyset$. Without loss of generality, we focus on validating the impact of knowledge transfer on \mathcal{P}_t to demonstrate that UniTrans has robust service support for hospitals with limited knowledge. Specifically, the goal of UniTrans is to enhance the task performance of \mathcal{P}_t 's local H_t^{nl} by transferring the knowledge from H_t^{ol} and H_d^{ol} . This significantly broadens the practical applicability of VFL in real-world scenarios.

IV. UNITRANS'S DESIGN

A. Overview

We demonstrate the overall process of UniTrans (Fig. 3). Note that before our mechanism runs, we suppose that overlapping IDs I_t^{ol} between \mathcal{P}_t and \mathcal{P}_d are known, which can be learned by private set intersection (PSI) methods [36]. Our framework can be simplified into three main steps (Fig. 4).

- **Step 1. Federated Representation Learning (FRL).** First, \mathcal{P}_t and \mathcal{P}_d collaboratively learn federated latent representations $H_{fed}^{ol} \in \mathbb{R}^{|I_t^{ol}| \times |X_t^\beta + X_d|}$ using secure VFL techniques. In brief, these federated latent representations would incorporate the hidden knowledge among multiple parties while not leaking these parties' raw data.
- **Step 2. Local Knowledge Transfer (LKT).** Second, \mathcal{P}_t trains a domain-adaptive representation transfer module

designed to transfer knowledge from federated latent representations, enriching the feature representations of local non-overlapping patients.

- **Step 3. Task-Specific Learning.** After Step 2, the LKT module is ready for local feature augmentation. With any given label Y_t^{nl} to predict, \mathcal{P}_t can leverage the enriched representations of local samples (i.e., original local features combined with the augmented representations) to perform training and inference using state-of-the-art (SOTA) machine learning (ML) algorithms.

Step 3 generally follows traditional supervised learning methods to train a task-specific prediction model, allowing the application of various ML algorithms, such as XGBoost [37] and VGG16 [38]. Next, we illustrate more details about Step 1 and 2. For simplicity, we begin by considering a scenario with a single \mathcal{P}_t and a single \mathcal{P}_d , which aligns with the common setup in VFL [35], [29]. At the end of Sec. IV-C, we will expand our discussion to address scenarios involving multiple data hospitals.

B. Federated Representation Learning

The objective of Step 1 is to extract federated latent representations H_{fed}^{ol} by leveraging H_t^{ol} and H_d^{ol} in a privacy-friendly manner. This step can utilize a range of vertical federated representation learning techniques to achieve effective feature extraction. In this work, we adopt a matrix decomposition-based federated representation method, as previous studies have demonstrated its effectiveness in extracting meaningful latent representations for ML tasks [39]. Specifically, we utilize two state-of-the-art federated matrix decomposition methods: FedSVD [26] and VFedPCA [40]. Below, we detail how these methods are modified and applied to learn H_{fed}^{ol} by incorporating H_t^{ol} and H_d^{ol} .

1) *FedSVD:* In FedSVD [26], \mathcal{P}_t and \mathcal{P}_d use two random orthogonal matrices to transform the H_t^{ol} and H_d^{ol} into masked \hat{H}_t^{ol} and \hat{H}_d^{ol} , respectively. This maintains the invariance of the decomposition results despite the masking transformation of the local samples. \hat{H}_t^{ol} and \hat{H}_d^{ol} are then uploaded to a third-party server, which applies the SVD algorithm to the masked patient samples from all hospitals. Finally, \mathcal{P}_t can reconstruct the federated latent representation based on the decomposition results.

Suppose \mathcal{P}_t holds the overlapping samples' feature matrix $H_t^{ol} \in \mathbb{R}^{|I_t^{ol}| \times |X_t^\beta|}$, and \mathcal{P}_d holds the overlapping samples' feature matrix $H_d^{ol} \in \mathbb{R}^{|I_d^{ol}| \times |X_d|}$ ($I_t^{ol} = I_d^{ol} = I_t \cap I_d$ is the overlapping sample ID set). Denote $H^{ol} = [H_t^{ol} | H_d^{ol}]$ (combination of both task and data hospitals' feature matrices), we want to leverage $H^{ol} = U\Sigma V^T$ (SVD) to learn the latent representations U . Inspired by FedSVD [26], we use a randomized masking method to learn U as:

- 1) A trusted key generator generates two randomized orthogonal matrices $A \in \mathbb{R}^{|I_t^{ol}| \times |I_t^{ol}|}$ and $B \in \mathbb{R}^{|X_{fed}^{ol}| \times |X_{fed}^{ol}|}$ ($|X_{fed}^{ol}| = |X_t^{ol}| + |X_d^{ol}|$). B is further partitioned to two parts $B_t \in \mathbb{R}^{|X_t^{ol}| \times |X_{fed}^{ol}|}$ and $B_d \in \mathbb{R}^{|X_d^{ol}| \times |X_{fed}^{ol}|}$, i.e., $B^T = [B_t^T | B_d^T]$.

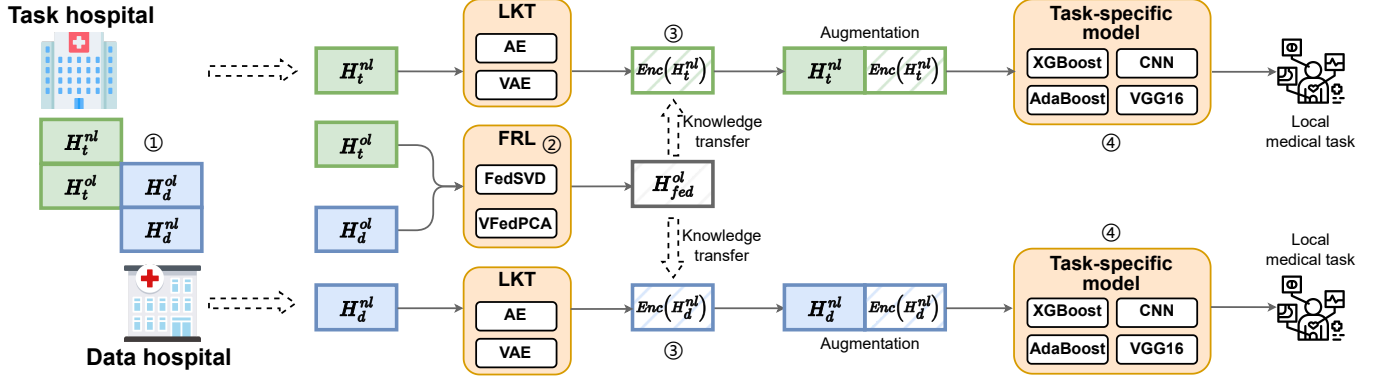


Fig. 3. Overview of UniTrans for two hospitals. Both \mathcal{P}_t and \mathcal{P}_d can benefit from UniTrans. ① \mathcal{P}_t and \mathcal{P}_d collaborate to identify overlapping samples H_t^{ol} and H_d^{ol} through PSI. ② With the assistance of a trusted third-party server, \mathcal{P}_t and \mathcal{P}_d conduct online FRL to generate the federated latent representation H_{fed}^{ol} , for the overlapping samples. ③ Using H_{fed}^{ol} , both \mathcal{P}_t and \mathcal{P}_d perform LKT offline to transfer knowledge to their respective local, non-overlapping samples, H_t^{nl} and H_d^{nl} . This step augments their local features. ④ With the augmented features, \mathcal{P}_t and \mathcal{P}_d can carry out their respective downstream prediction tasks according to their individual requirements.

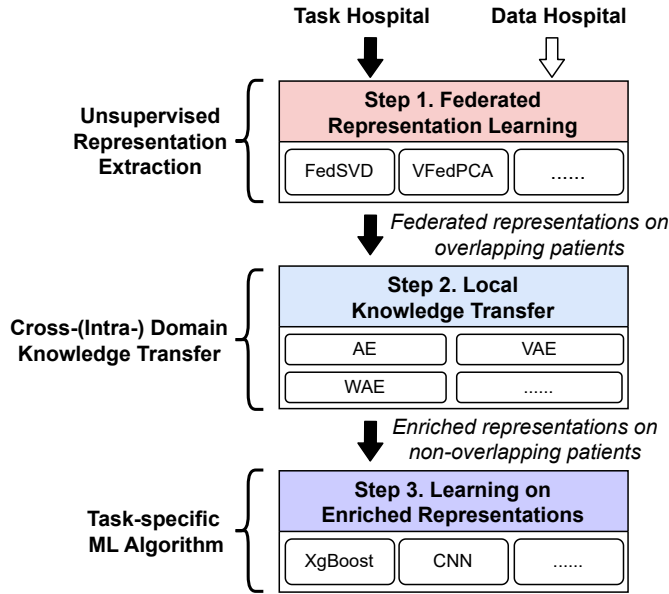


Fig. 4. Overview of UniTrans.

- 2) A and B_t are sent to \mathcal{P}_t ; A and B_d are sent to \mathcal{P}_d . Each hospital does a local computation by masking its own original feature matrices with the received matrices:

$$\hat{H}_k^{ol} = AH_k^{ol}B_k, \forall k \in \{t, d\} \quad (1)$$

- 3) \mathcal{P}_t and \mathcal{P}_d send \hat{H}_t^{ol} and \hat{H}_d^{ol} respectively to a third-party server² and the third-party server runs SVD on the combined data matrix $\hat{H}^{ol} = \hat{U}\Sigma\hat{V}^T$, where $\hat{H}^{ol} = [\hat{H}_t^{ol}|\hat{H}_d^{ol}]$. \hat{U} is then sent back to \mathcal{P}_t .
- 4) \mathcal{P}_t can recover the federated latent representation of shared samples, denoted as H_{fed}^{ol} , by

$$H_{fed}^{ol} = U = A^T\hat{U} \quad (2)$$

²The third-party server needs to be semi-honest. Note that in FL, such a security configuration (i.e., the information aggregation server is semi-honest) is widely accepted [41].

Compared to the original FedSVD which aims to recover both U and V [26], we only need to recover U . Hence, in UniTrans, only \hat{U} is transmitted to \mathcal{P}_t to reduce the communication cost. The correctness of the above process depends on the fact that H^{ol} and \hat{H}^{ol} (multiplying H^{ol} by two orthogonal matrices) must hold the same singular value Σ [26].

2) *VFedPCA*: To enhance the generality of UniTrans, we also use vertical federated principal component analysis (VFedPCA) [40] to extract latent representations. Under VFedPCA's setting, each hospital makes its own federated eigenvector u converge to global eigenvector u_G without needing to know the mutual data of all hospitals. Each hospital is able to train the local eigenvector using local power iteration [42]. Then the eigenvectors from each hospital are merged into the federated eigenvector u . Finally, \mathcal{P}_t can use u to reconstruct the original data to obtain the federated latent representation.

Suppose \mathcal{P}_t holds $H_t^{ol} \in \mathbb{R}^{|I_t^{ol}| \times |X_t^{ol}|}$, and \mathcal{P}_d holds $H_d^{ol} \in \mathbb{R}^{|I_d^{ol}| \times |X_d^{ol}|}$. Denote $H^{ol} = [H_t^{ol}|H_d^{ol}]$

- 1) For each hospital $k \in \{t, d\}$, we calculate the largest eigenvalue $A_k = \frac{1}{|X_k|} (H_k^{ol})^T H_k^{ol}$ and a non-zero vector a_k corresponding to the eigenvector $\delta_k (A_k a_k = \delta_k a_k)$. The number of local iterations is L , each hospital will compute locally until convergence as follows:

$$a_k^l = \frac{A_k a_k^{l-1}}{\|A_k a_k^{l-1}\|}, \quad \delta_k^l = \frac{A_k (a_k^l)^T a_k^l}{(a_k^l)^T a_k^l} \quad (3)$$

where $l = 1, 2, \dots, L$.

- 2) Then each hospital upload the eigenvector a_k^L and the eigenvalue δ_k^L to third-party server. The server aggregates the results and generates the federated eigenvalue:

$$u = \sum_{k \in \{t, d\}} w_k a_k^L, \quad w_k = \frac{\delta_k^L}{\sum_{k \in \{t, d\}} \delta_k^L} \quad (4)$$

- 3) \mathcal{P}_t can use the federated eigenvalue u to reach the H_{fed}^{ol} :

$$H_{fed}^{ol} = H_t^{ol} \frac{MM^T}{\|MM^T\|}, \quad M = (H_t^{ol})^T u \quad (5)$$

C. Local Knowledge Transfer

After obtaining H_{fed}^{ol} for overlapping samples, Step 2 aims to enrich the \mathcal{P}_t 's non-overlapping samples' representations. The overlapping and non-overlapping samples of \mathcal{P}_t may come from different domains, resulting in feature heterogeneity or label heterogeneity. However, existing knowledge transfer techniques in VFL are unable to address this challenge. Some studies have demonstrated that cross-attention mechanisms [43] can facilitate better feature alignment in domain adaptation [44], [45] and domain generalization [46], [47]. Building on these concepts, we developed a domain-adaptive unified knowledge transfer module utilizing a cross-attention mechanism. This module is designed with two primary objectives: ① fuse invariant features between source domain and target domain in the same subspace, and ② perform label-free knowledge transfer.

For the patients' data H_t^{nl} , we use an auto-encoder $Enc-Dec$ to extract representations $Enc(H_t^{nl})$. We then employ a cross-attention mechanism to learn domain-invariant features Z_t^{nl} :

$$\begin{aligned} Z_t^{nl} &= \text{attn}(Enc(H_t^{nl}), H_{fed}^{ol} \otimes \Phi) \\ &= \text{softmax}\left(\frac{Enc(H_t^{nl}) \otimes (H_{fed}^{ol} \otimes \Phi)^T}{\sqrt{X_t^{nl}}}\right) \otimes (H_{fed}^{ol} \otimes \Phi) \end{aligned} \quad (6)$$

where Φ is a learnable parameter matrix of dimension $X_{fed}^{ol} \times X_t^{nl}$ to capture β -to- α cross domain transformation. In this way, we transform the learned global federated knowledge into local knowledge.

To enhance knowledge transfer, we employ a Mutual Information Neural Estimator (MINE) [48] to maximize the mutual information between the target domain representations $P = Enc(H_t^{nl})$ and the transferred domain-invariant representations $Q = Z_t^{nl}$. To avoid integral computation, we use Monte-Carlo integration to estimate mutual information:

$$MI(P, Q) = \frac{1}{N} \sum_{i=1}^N I(p, q, \theta) - \log\left(\frac{1}{N} \sum_{i=1}^N e^{I(p, q', \theta)}\right) \quad (7)$$

where (p, q) is sampled from the joint distribution, q' is sampled from the marginal distribution, and I is a neural network with parameters θ used to estimate the mutual information between P and Q . We incorporate the mutual information $\mathcal{L}_{mi} = MI(P, Q)$ estimated by MINE into the loss function to enhance the valuable information between the source and target domains. Hence, the complete loss function of the LKT module is:

$$\mathcal{L} = \mathcal{L}_{recons} - \lambda \mathcal{L}_{mi} \quad (8)$$

The process of LKT is shown in Fig. 5.

Extension to multiple data hospitals. When there are n data hospitals, the \mathcal{P}_t can repeat the aforementioned Step 1 and 2 with each $\mathcal{P}_{d,i}$. Specifically, for each data hospital $\mathcal{P}_{d,i}$, \mathcal{P}_t can learn a local feature extractor Enc_i . Then, by aggregating n local feature extractors learned from n data hospitals, the local samples' final enriched representations of \mathcal{P}_t become,

$$\tilde{H}_t^{nl} = \langle H_t^{nl}, Enc_1(H_t^{nl}), \dots, Enc_n(H_t^{nl}) \rangle \quad (9)$$

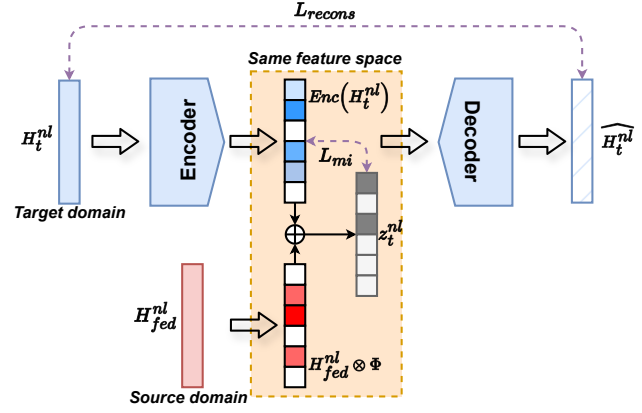


Fig. 5. The process of LKT of UniTrans.

Our mechanism allows the \mathcal{P}_t to perform FRL and LKT with each $\mathcal{P}_{d,i}$ to obtain enhanced representations. These enhanced representations are concatenated with the H_t^{nl} to obtain the final enhanced representations \tilde{H}_t^{nl} . However, as the number of data hospitals increases, the concatenated representations grow, leading to significant redundant knowledge. To address this challenge, we fine-tune each Enc_i based on contrastive learning. For each \mathcal{P}_t - $\mathcal{P}_{d,i}$ pair, we minimize the distance between $Enc_i(H_t^{nl})$ and $Z_{t,i}^{nl}$ while maximize the distance between $Enc_i(H_t^{nl})$ and $\{Z_{t,k}^{nl}; k \in n, k \neq i\}$ from other data hospitals:

$$\mathcal{L}_{cl} = -\log \frac{\exp(\text{Dist}(Enc_i(H_t^{nl}), Z_{t,i}^{nl})/\tau)}{\sum_{k=1}^n \exp(\text{Dist}(Enc_k(H_t^{nl}), Z_{t,k}^{nl})/\tau)} \quad (10)$$

where τ is a temperature coefficient. The goal of this approach is to enable each Enc_i to learn unique representations from the view of \mathcal{P}_t and $\mathcal{P}_{d,i}$, thereby reducing redundant knowledge.

The procedure steps of UniTrans can be found in Alg. 1.

D. Security and Privacy

Security and privacy are key factors to consider in FL mechanism design. While UniTrans is a knowledge transfer framework that incorporates existing VFL algorithms, the security and privacy protection levels are mainly dependent on the included VFL algorithm. In particular, the FRL module (Sec. IV-B) is the key part to determine the overall security and privacy levels of UniTrans, as cross-party communications and computations are only conducted in this step. Currently, we implement the FRL module with SOTA VFL representation learning methods including, FedSVD [26] and VFedPCA [40]. FedSVD uses two random orthogonal matrices to mask the original data. The third-party server can only use the masked data of each party to obtain SVD result. The third-party server of VFedPCA only needs to use the eigenvectors and eigenvalues of each party's data for weighted summation. All of these methods protect privacy by preventing direct use of data by non-holders. Due to the page limitation, readers may refer to the original papers [26], [40] for specific security and privacy analysis.

Algorithm 1 UniTrans mechanism

```

1: function FRL( $H_t, H_d$ )
2:    $H_t^{ol}, H_d^{ol} \leftarrow PSI(H_t, H_d)$ 
3:    $H_{fed}^{ol} \leftarrow FedSVD(H_t^{ol}, H_d^{ol})$ 
4:   Return  $X_{fed}^{ol}$ 
5: end function

6: function LKT( $H_t, H_{d1}, H_{d2}, \dots, H_{dn}$ )
7:   ① Model Training
8:   for  $i$  in range( $n$ ) do
9:     Initialize an auto-encoder  $Enc_i-Dec_i$ 
10:    Initialize  $\Phi_i$ 
11:     $H_{fed,i}^{ol} \leftarrow FRL(H_t, H_{di})$ 
12:    while stopping epoch not met do
13:       $Z_{t,i}^{nl} = attn(Enc_i(H_t^{nl}), H_{fed,i}^{ol} \otimes \Phi_i)$ 
14:       $\mathcal{L}_{recons} = \|H_t^{ol} - Dec_i(Enc_i(H_t^{nl}))\|_2$ 
15:       $\mathcal{L}_{mi} = MI(Enc_i(H_t^{nl}), Z_{t,i}^{nl})$ 
16:       $\mathcal{L} = \mathcal{L}_{recons} - \lambda \mathcal{L}_{mi}$ 
17:       $Enc_i-Dec_i \leftarrow Backward(\mathcal{L})$ 
18:       $\Phi_i \leftarrow Backward(\mathcal{L})$ 
19:    end while
20:  end for
21:  ② Model Fine-tuning
22:  for  $i$  in range( $n$ ) do
23:     $Z_{t,i}^{nl} = attn(Enc_i(H_t^{nl}), H_{fed,i}^{ol} \otimes \Phi_i)$ 
24:    while stopping epoch not met do
25:       $\mathcal{L}_{cl} = CL(Enc_i(H_t^{nl}), Z_{t,i}^{nl})$ 
26:       $Enc_i \leftarrow Backward(\mathcal{L}_{cl})$ 
27:    end while
28:  end for
29:  ③ Feature Augmentation
30:   $\tilde{H}_t^{nl} \leftarrow \langle H_t^{nl}, Enc_1(H_t^{nl}), \dots, Enc_n(H_t^{nl}) \rangle$ 
31:  Return  $\tilde{H}_t^{nl}$ 
32: end function

```

E. Updating

In general, UniTrans is efficient to update without the need to completely re-running three steps for all the hospitals.

Local Incremental Learning - *New task samples.* UniTrans trains a dedicated LKT for local samples from each target domain. When new samples are introduced, \mathcal{P}_t can directly apply the pre-trained LKT for efficient knowledge transfer, eliminating the need for retraining or further communication with other data hospitals.

Task Independence - *New tasks.* Similar to new samples, if \mathcal{P}_t has a new task label to predict, \mathcal{P}_t also does not need to communicate with other hospitals. \mathcal{P}_t can simply repeat Step 3 of UniTrans using the new task label, ensuring adaptability to evolving prediction requirements.

Knowledge Extensibility - *New data hospitals.* \mathcal{P}_t can learn a new local feature enrichment function Enc from the new \mathcal{P}_d (repeat Steps 1 and 2 with the new \mathcal{P}_d), and then enrich the representation as $\tilde{H}_t^{nl} = \langle \tilde{H}_t^{nl}, Enc(H_t^{nl}) \rangle$.

V. EVALUATION

Our experiments were performed on the workstation using NVIDIA RTX 4090, Intel Xeon(R) Gold 6430, 128GB RAM,

PyTorch 1.10.0, Python 3.8 and CUDA 12.0.

A. Evaluation Setup

Datasets and Partitions. We evaluate UniTrans on the seven medical datasets:

- *Medical Information Mart for Intensive Care Dataset (MIMIC-III)* [49] provides de-identified health-related data for 58,976 patients with 15 pieces of health information as features from 2001 to 2012. Length of stays is the target of prediction and varies between 1 and 4.
- *Cardiovascular Disease Dataset (Cardio)* [50] consists of 70,000 patient records, each containing 11 features. The labels 1 and 0 indicate the presence or absence of cardiovascular disease, respectively.
- *Gene Expression Cancer RNA Sequence Dataset (RNA-Seq)* [51] contains gene expression data from patients with various tumor types. It has a dimension of $801 \times 20,531$, with five tumor types as prediction targets. Each sample’s features represent RNA-Seq gene expression levels.
- *Heart Attack Risk Prediction Dataset (Heart)* [52] is synthetic and includes 26 features associated with heart health and lifestyle choices for 8,763 patients. Labels 1 and 0 indicate whether a patient is at risk of a heart attack or not, respectively.
- *Prediction of Sepsis Dataset (Sepsis)* [53] includes 17 clinical and laboratory features from 45,852 patients. The task is to predict sepsis six hours before its clinical onset. A label of 1 indicates an impending sepsis event, while 0 signifies no risk.
- *Leukemia Classification (Leukemia) dataset* [54] contains 15,135 images from 118 patients with two label: 0 for normal cell and 1 for leukemia cell.
- *Chest X-Ray Images (Pneumonia) dataset* [55] contains 5,863 X-ray images and 2 classes (pneumonia/normal).

The used datasets have been widely used in previous FL-empowered healthcare studies [5], [56], [57]. The dataset summary and detailed data partitions is provided in Appendix. We assume a scenario with one \mathcal{P}_t and one \mathcal{P}_d by default, which aligns with the standard setup in VFL [35], [29]. The five datasets—MIMIC-III, Cardio, RNA-Seq, Heart, and Sepsis—are utilized to evaluate the effectiveness of intra-domain knowledge transfer. The two datasets, Leukemia and Pneumonia, are used to assess the performance of cross-domain knowledge transfer. In the intra-domain setting, both H_t^{nl} and H_t^{ol} are derived from the same domain, share an identical feature space, and are randomly sampled from the original dataset. Following the existing cross-domain settings [58], [59], we define the target domain data, H_t^{nl} , as cropped images focusing on the central area, while the source domain data, H_t^{ol} , consists of complete images. During data partition, the target domain is assigned two types of labels, whereas the source domain retains a single type of label.

Baselines. To verify the effectiveness of our mechanism, we compare with six baselines:

- *Local:* This baseline leverages only the \mathcal{P}_t ’s local non-overlapping H_t^{nl} for training the task-specific prediction.

- *FTL [60]*: FTL is an end-to-end FL method for transferring knowledge to local samples. Specifically, based on shared samples, FTL maps different parties' raw features to a common feature space to achieve knowledge transfer.
- *VFL-Infer [8]*: VFL-Infer first learns a federated model on shared samples and then learns a local model (for local samples) by considering both ground-truth labels and soft labels produced by the federated model.
- *FedCVT [9]*: FedCVT leverages existing representations to estimate missing features for \mathcal{P}_t and generates pseudo-labels for unlabeled samples, thereby creating an expanded training dataset.
- *FedHSSL [10]*: FedHSSL first uses cross-party SSL to train a cross-party encoder on H_t^{ol} and H_d^{ol} , and then uses the cross-party encoder to train a local encoder on H_t^{ol} and H_t^{nl} to perform augmentation.
- *VFedTrans [5]*: VFedTrans [5] facilitates knowledge transfer in a task-independent manner through local representation distillation.

The default settings for these baselines follow the configuration used in the original paper. While FTL, VFL-Infer, FedCVT, FedHSSL, and VFedTrans can be used to assist local non-overlapping samples' learning in VFL, they do not address two key challenges: feature heterogeneity (FH) and label heterogeneity (LH).

Training Setup. UniTrans's training involves three main modules: the FRL module, the LKT module, and task-specific models.

FRL modules. We use two VFL techniques, FedSVD and VFedPCA, FedSVD and VFedPCA, with FedSVD as the default method. We set `block_size` to 100 in FedSVD. For VFedPCA, we configure `iter_num` to 100, `period_num` to 10, and `warm_start` to True.

LKT modules. For the LKT modules, we use the Adam optimizer [61] with the following settings: `learning_rate` = 0.001, `batch_size` = 100, and 30 epochs. We use $\beta_0 = 1e - 3$ and $\beta_1 = 1e - 1$ to balance \mathcal{L}_{recons} and \mathcal{L}_{mi} . The default LKT method is the vanilla Auto-Encoder (AE). Additionally, we conduct experiments with alternative LKT methods, including Variational Auto-Encoder (VAE) [62] and Wasserstein Auto-Encoder (WAE) [63], to assess the robustness of our framework. The key parameters for these three modules are summarized in Appendix.

Task-specific models. For all the datasets, when training the task-specific model, we choose 80% of H_t^{nl} as the training set and 20% as the test set. In order to prevent the interference of random seeds, we carry out experiments under 10 different random seeds and compute the average prediction results.

Note that traditional ML models often perform efficiently and effectively in many medical tasks [64]. In our experiments, we use the XGBoost [37] and Convolutional Neural Networks (CNN) [65] as the default algorithm. We also test the other popular algorithms, including Adaboost [66], multi-Layer perceptron (MLP), TabNet [67] and VGG16 [38] for robustness checks in Sec. V-E. For XGBoost and Adaboost, we use grid search to find the optimal parameters. The parameters of the rest downstream model are summarized in Appendix.

We evaluate UniTrans by addressing the following key research questions:

- **RQ1.** How effective is UniTrans's intra-domain knowledge transfer?
- **RQ2.** How effective is UniTrans's cross-domain knowledge transfer?
- **RQ3.** How does UniTrans perform in a few-shot scenario with limited training data?
- **RQ4.** Can UniTrans achieve strong performance on different FRL, LKT modules and downstream ML methods?
- **RQ5.** How does UniTrans's prediction performance for non-overlapping patients and system efficiency change as the number of data hospitals increases?

B. Intra-domain Main Evaluations

We first verify the effectiveness of UniTrans in intra-domain knowledge transfer. Fig. 6 depicts the prediction performance on five datasets by varying the number of features in \mathcal{P}_t . Intra-domain learning requires that the input dimensions of the data are consistent, so the feature dimensions of H_t^{ol} and H_t^{nl} will change synchronously. The results show that as the feature scale of \mathcal{P}_t increases, the prediction accuracy of all methods improves. Due to more effective intra-domain knowledge transfer, UniTrans achieves the highest accuracy. It is worth noting that when the number of features is relatively low, existing baselines struggle to make effective predictions. However, the feature augmentation strategy provided by UniTrans enhances prediction performance and is particularly beneficial for hospitals with limited medical resources.

Fig. 7 illustrates the prediction performance across five datasets as the number of features in \mathcal{P}_d is varied. The accuracy of UniTrans consistently improves as the number of features in \mathcal{P}_d increases. Notably, UniTrans achieves higher classification accuracy compared to the baselines, suggesting that it can transfer knowledge from the rich feature set of \mathcal{P}_d more efficiently.

Fig. 8 shows how our mechanism performs by changing the number of overlapping samples between \mathcal{P}_t and \mathcal{P}_d . We observe that the performance gets better as there are more shared samples. This also validates the effectiveness of UniTrans: with more knowledge sources (i.e., shared samples), our transfer can always be better.

Answer to RQ1: UniTrans effectively transfers cross-party knowledge to non-overlapping samples within the domain. As the knowledge base grows, UniTrans improves its ability to make more accurate predictions for downstream tasks.

C. Cross-domain Main Evaluations

Then we verify the effectiveness of UniTrans in cross-domain knowledge transfer. As discussed in Sec. I, cross-domain scenarios present significant challenges, including feature heterogeneity and label heterogeneity. To thoroughly assess UniTrans, we separately validate its performance under each of these heterogeneous scenarios.

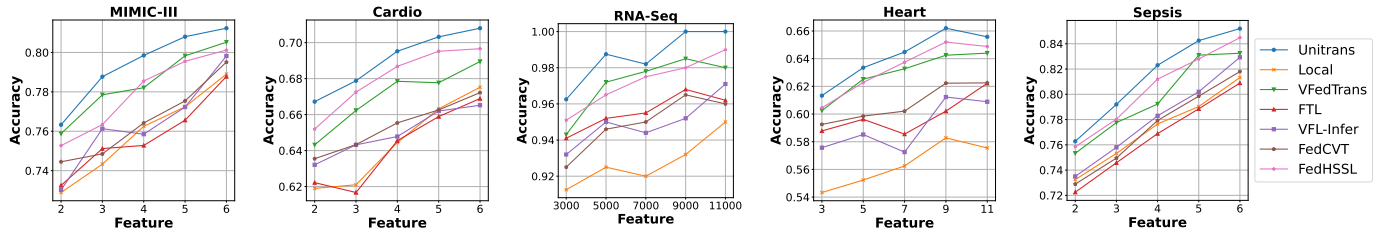


Fig. 6. Prediction accuracy by varying the feature numbers of \mathcal{P}_t .

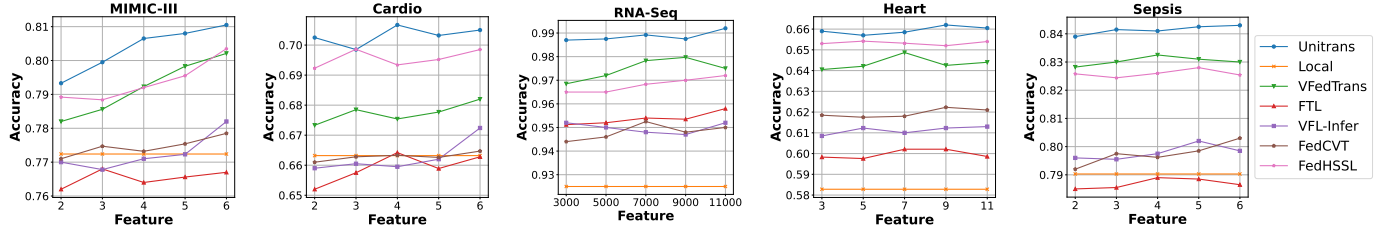


Fig. 7. Prediction accuracy by varying the feature numbers of \mathcal{P}_d .

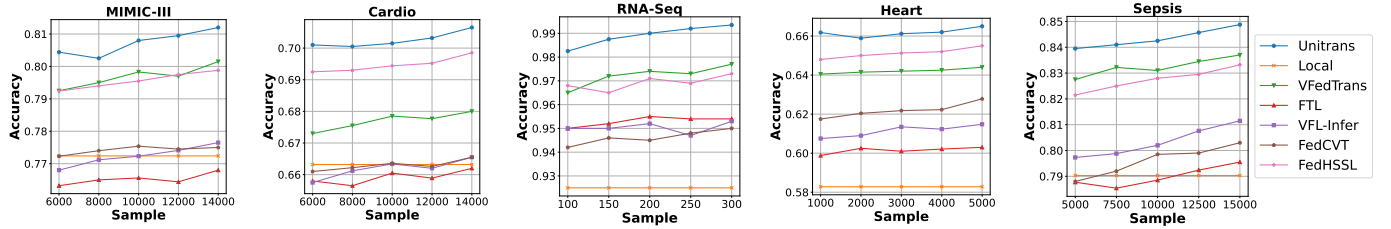


Fig. 8. Prediction accuracy by varying the number of overlapping samples between \mathcal{P}_t and \mathcal{P}_d .

Feature Heterogeneity. As shown in Tbl. I, among the existing methods, only FTL is capable of addressing feature heterogeneity. To evaluate the effectiveness of UniTrans in this context, we compare its downstream task prediction performance against Local and FTL approaches on the Leukemia and Pneumonia datasets. Fig. 9 illustrates the prediction performance across various target domain image sizes. The results demonstrate that UniTrans consistently achieves the highest prediction accuracy. Notably, when the target domain image size is small (indicating insufficient knowledge), UniTrans significantly enhances the target domain’s prediction performance. This highlights UniTrans’s robustness and effectiveness in scenarios with limited knowledge. Fig. 10 evaluates the impact of varying the amount of source domain data on the prediction performance in the target domain. The results indicate that as the volume of source domain data increases, both UniTrans and FTL contribute to improving the prediction accuracy of the target domain. However, UniTrans consistently facilitates the most significant performance enhancement during the knowledge transfer process.

Label Heterogeneity. Among existing methods, VFedTrans and FedHSSL address the issue of label heterogeneity by ensuring that label information from the source domain is not included during knowledge transfer. As shown in Tbl. II, UniTrans excels in scenarios involving heterogeneous labels, achieving the best prediction performance without being affected by label heterogeneity. In contrast, methods like FTL, VFL-Infer, and FedCVT struggle to handle this scenario, leading to a marked decline in their prediction accuracy.

This demonstrates UniTrans’s robustness in challenging cross-domain environments with label heterogeneity.

TABLE II
PREDICTION ACCURACY IN SCENARIOS WITH HETEROGENEOUS LABELS.

†Method	Leukemia	Pneumonia
UniTrans	0.8048	0.9022
VFedTrans	0.7924	0.8923
Local	0.7812	0.8884
FTL	0.6785	0.7243
VFL-Infer	0.6229	0.7021
FedCVT	0.7024	0.7435
FedHSSL	0.7984	0.8965

Answer to RQ2: UniTrans demonstrates superior performance in cross-domain knowledge transfer by effectively addressing both feature heterogeneity and label heterogeneity.

D. Few-Shot Evaluation

In real-world scenarios, data holders often possess predominantly unlabeled data with access to only a few labeled samples. This is particularly true for rare medical conditions, where the scarcity of labeled instances creates imbalanced datasets with limited training examples. To evaluate performance under these conditions, we simulate a few-shot learning setting where \mathcal{P}_t has access to only 10% of the original labeled samples for training the downstream model. Tbl. III summarizes the results under this constrained setting. The results indicate that the prediction performance of all methods

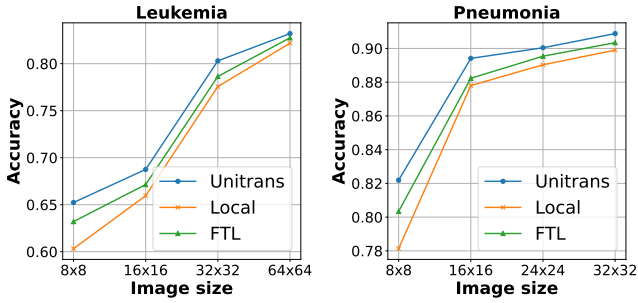


Fig. 9. Prediction accuracy of the target domain at different image sizes.

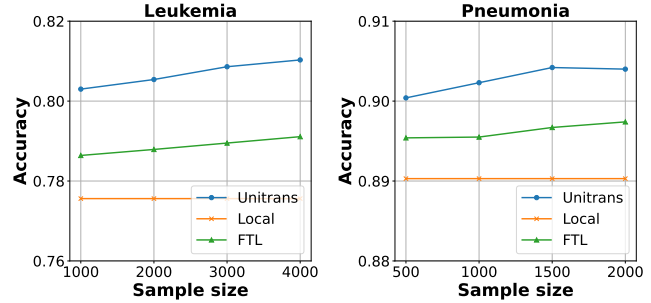


Fig. 10. Prediction accuracy of the target domain at different sample sizes.

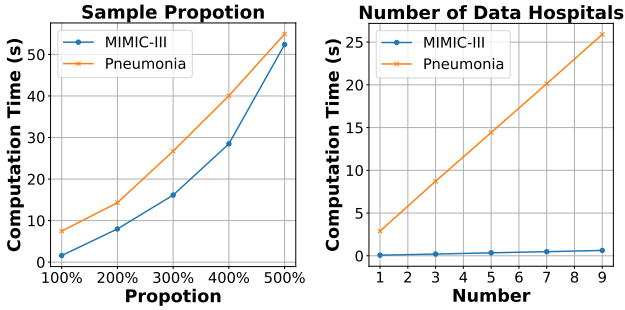


Fig. 11. Computation time by varying the number of \mathcal{P}_{ds} and the number of overlapping samples.

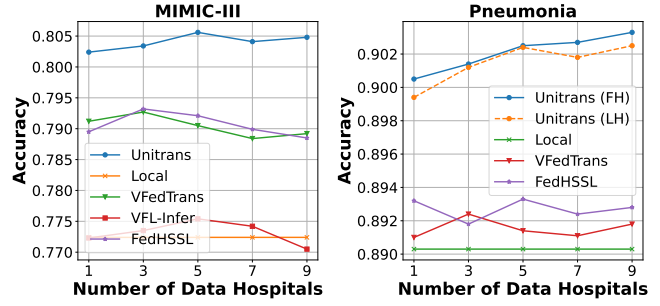


Fig. 12. Prediction accuracy by increasing the number of \mathcal{P}_{ds} .

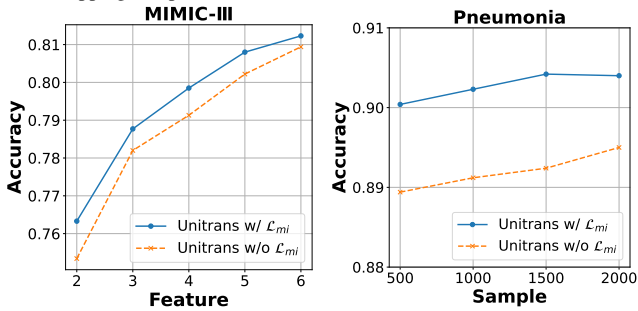


Fig. 13. Prediction accuracy of MIMIC-III and Pneumonia with or without \mathcal{L}_{mi} .

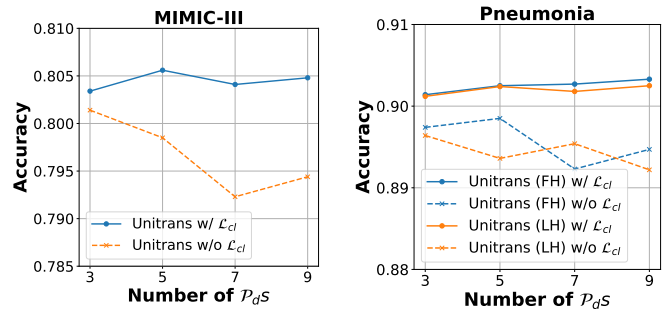


Fig. 14. Prediction accuracy by varying number of \mathcal{P}_{ds} with or without \mathcal{L}_{cl} .

declines to some extent due to the lack of labeled data. However, UniTrans demonstrates a significant advantage, consistently outperforming other methods on seven datasets. This highlights UniTrans’s robustness and efficiency in extracting and utilizing knowledge even in few-shot scenarios, making it well-suited for real-world applications with limited labeled data.

Answer to RQ3: UniTrans excels in few-shot scenarios by consistently outperforming other methods, demonstrating its ability in leveraging limited labeled data for real-world applications.

E. Robustness Evaluation

Here, we assess the robustness of UniTrans by modifying its configurations, including the FRL and LKT modules, as well as the downstream machine learning methods.

Tbl. IV and V present the results when UniTrans employs different ML models to train the task classifier. UniTrans consistently outperforms the baseline across various ML methods, demonstrating the wide-ranging effectiveness

of our knowledge transfer approach across different datasets and models. This also highlights the flexibility of UniTrans, which accommodates the use of any classification model. Such flexibility is especially beneficial in practical medical scenarios, as it enables the classifier to better align with the specific characteristics of the target patients.

Additionally, we evaluate the impact of changing the modules in the FRL and LKT modules of UniTrans and VFedTrans. For the FRL module, we experimented with FedSVD [26] and VFedPCA [40]. For the LKT module, we used vanilla AE, VAE and WAE. Tbl. VI summarize the prediction accuracy for different module configurations. The results show that the final accuracy remains robust to these modifications.

Answer to RQ4: UniTrans demonstrates exceptional robustness and flexibility, consistently outperforming baselines across diverse ML models, datasets, and module configurations, highlighting its adaptability and effectiveness in practical scenarios such as medical applications.

TABLE III
PREDICTION ACCURACY UNDER FEW-SHOT SETTING.

†Method	MIMIC-III	Cardio	RNA-Seq	Heart	Sepsis	Leukemia		Pneumonia	
						FH	LH	FH	LH
UniTrans	0.8023	0.6364	0.8243	0.6526	0.7025	0.7964	0.7969	0.8859	0.8922
Local	0.7721	0.6022	0.7984	0.5522	0.6884	0.7538	0.7605	0.8678	0.8763
VFedTrans	0.7944	0.6224	0.8122	0.6175	0.6954	-	0.7896	-	0.8805
FTL	0.7956	0.6229	0.8089	0.6324	0.6969	0.7843	0.6243	0.8787	0.6889
VFL-Infer	0.7702	0.6178	0.8024	0.6102	0.6844	-	0.6187	-	0.6774
FedCVT	0.7733	0.6240	0.8075	0.6074	0.6903	-	0.6785	-	0.7320
FedHSSL	0.7924	0.6309	0.8188	0.6420	0.6987	-	0.7920	-	0.8867

TABLE IV
CROSS-DOMAIN PREDICTION ACCURACY UNDER DIFFERENT DOWNSREAM MODELS.

†Method	Leukemia		Pneumonia	
	FH	LH	FH	LH
UniTrans (CNN)	0.8030	0.8048	0.9023	0.9022
VFedTrans (CNN)	-	0.7924	-	0.8923
Local (CNN)	0.7756	0.7812	0.8903	0.8884
UniTrans (VGG16)	0.8053	0.8064	0.8995	0.8981
VFedTrans (VGG16)	-	0.7904	-	0.8867
Local (VGG16)	0.7812	0.7803	0.8885	0.8892
FTL	0.7864	0.6785	0.8955	0.7243
VFL-Infer	-	0.6229	-	0.7021
FedCVT	-	0.7024	-	0.7435
FedHSSL	-	0.7984	-	0.8965

TABLE V
INTRA-DOMAIN PREDICTION ACCURACY UNDER DIFFERENT DOWNSREAM MODELS.

†Method	MIMIC-III	Cardio	RNA-Seq	Heart	Sepsis
UniTrans (XGBoost)	0.8080	0.7132	0.9875	0.6620	0.8425
VFedTrans (XGBoost)	0.7983	0.6777	0.9720	0.6425	0.8310
Local (XGBoost)	0.7724	0.6632	0.9250	0.5828	0.7903
UniTrans (AdaBoost)	0.7942	0.7150	0.9820	0.6589	0.8386
VFedTrans (AdaBoost)	0.7785	0.7065	0.9750	0.6407	0.8295
Local (AdaBoost)	0.7533	0.6604	0.9284	0.5850	0.7854
UniTrans (FCNN)	0.8025	0.7035	0.9935	0.6612	0.8395
VFedTrans (FCNN)	0.7910	0.6873	0.9837	0.6427	0.8344
Local (FCNN)	0.7625	0.6578	0.9364	0.5835	0.7866
UniTrans (TabNet)	0.7983	0.6972	0.9915	0.6592	0.8403
VFedTrans (TabNet)	0.7830	0.6825	0.9806	0.6388	0.8330
Local (TabNet)	0.7675	0.6535	0.9325	0.5815	0.7890
FTL	0.7656	0.6589	0.9520	0.6021	0.7885
VFL-Infer	0.7723	0.6620	0.9500	0.6123	0.8020
FedCVT	0.7754	0.6626	0.9460	0.6223	0.7985
FedHSSL	0.7955	0.6952	0.9650	0.6520	0.8280

F. Scalability Evaluation

In real-world scenarios, \mathcal{P}_t may collaborate with multiple \mathcal{P}_d s to enhance local medical prediction services. As the number of \mathcal{P}_d s increases, the knowledge transfer method must satisfy two key conditions: ① Computational Efficiency: The process of transferring knowledge from each \mathcal{P}_d must remain computationally efficient. ② Knowledge Integration: It must effectively acquire knowledge from different \mathcal{P}_d s.

Computational Efficiency. The computational burden of UniTrans primarily depends on the FRL module, as this is the only step that involves collaboration between \mathcal{P}_t and \mathcal{P}_d . It is

important to note that our implemented FRL algorithm, such as FedSVD, is highly efficient and can be applied to feature matrices at a billion-scale [26]. This significantly contributes to the overall computational efficiency of UniTrans. We first evaluate the computational efficiency by varying the sample size of H_t^{ol} on MIMIC-III and Cardio datasets. Using the sample size in the default experimental settings as the lower limit (100%), we test how UniTrans performs with sample sizes ranging from 100% to 500%. The left graph of Fig. 11 illustrates that as the size of overlapping samples increases, the computational overhead for UniTrans remains low and shows only a minimal increase. Next, we assess the computational efficiency of UniTrans under scenarios involving multiple \mathcal{P}_d s. Unlike HFL, the number of participants in VFL is typically limited to single digits. As shown in the right graph of Fig. 11, the computational overhead of UniTrans increases linearly with the number of \mathcal{P}_d s. This linear relationship demonstrates the scalability and efficiency of our mechanism in handling additional participants.

Knowledge Integration. As the number of \mathcal{P}_d s increases, effectively transferring knowledge from multiple sources to H_t^{nl} becomes a significant challenge. To evaluate the ability of UniTrans to aggregate multi-party knowledge, we vary the number of \mathcal{P}_d s from 1 to 9 with a step size of 2. The evaluation results are shown in Fig. 12. Among the existing methods, FTL and FedCVT are limited to 2-party scenarios, which restricts their applicability in real-world settings. As the number of \mathcal{P}_d s increases, the marginal improvement in predictive performance from richer knowledge becomes limited. Methods such as VFedTrans, VFL-Infer, and FedHSSL experience a decrease in prediction accuracy under these conditions. In contrast, UniTrans is able to learn non-redundant knowledge, allowing it to maintain high prediction accuracy even with an increasing number of data hospitals.

Answer to RQ5: Our approach, UniTrans, demonstrates superior scalability by maintaining efficient knowledge transfer handling multiple \mathcal{P}_d s, ensuring high prediction accuracy even as the number of \mathcal{P}_d s grows.

G. Ablation Study

To further validate the effectiveness of UniTrans in knowledge transfer, we compare the changes in prediction accuracy before and after incorporating \mathcal{L}_{mi} . As shown in Fig. 13, the prediction accuracy improves significantly when \mathcal{L}_{mi} is

TABLE VI
PREDICTION ACCURACY BY CHANGING FRL AND LKT MODULES.

†Method	FRL	LKT	MIMIC-III	Cardio	RNA-Seq	Heart	Sepsis	Leukemia		Pneumonia	
								FH	LH	FH	LH
UniTrans	FedSVD	AE	0.8080	0.7132	0.9875	0.6620	0.8425	0.8030	0.8048	0.9023	0.9022
	FedSVD	VAE	0.8065	0.7122	0.9850	0.6634	0.8417	0.8011	0.8019	0.8996	0.9005
	FedSVD	WAE	0.8089	0.7105	0.9870	0.6615	0.8432	0.8025	0.7980	0.9010	0.9015
	VFedPCA	AE	0.8058	0.7129	0.9820	0.6609	0.8388	0.7988	0.7992	0.8978	0.8982
	VFedPCA	VAE	0.8065	0.7095	0.9840	0.6613	0.8397	0.7982	0.7978	0.8984	0.8990
	VFedPCA	WAE	0.8048	0.7102	0.9830	0.6578	0.8390	0.7994	0.8004	0.8988	0.8995
VFedTrans	FedSVD	AE	0.7983	0.6777	0.9720	0.6425	0.8310	-	0.7924	-	0.8923
	FedSVD	VAE	0.8005	0.6754	0.9740	0.6402	0.8344	-	0.7912	-	0.8905
	FedSVD	WAE	0.7975	0.6768	0.9710	0.6434	0.8353	-	0.7895	-	0.8912
	VFedPCA	AE	0.7965	0.6745	0.9765	0.6389	0.8295	-	0.7940	-	0.8893
	VFedPCA	VAE	0.7957	0.6712	0.9718	0.6394	0.8288	-	0.7902	-	0.8905
	VFedPCA	WAE	0.7975	0.6726	0.9685	0.6412	0.8308	-	0.7895	-	0.8885
Local	-	-	0.7724	0.6632	0.9250	0.5828	0.7903	0.7756	0.7812	0.8903	0.8884
FTL	-	-	0.7656	0.6589	0.9520	0.6021	0.7885	0.7864	0.6785	0.8955	0.7243
VFL-Infer	-	-	0.7723	0.6620	0.9500	0.6123	0.8020	-	0.6229	-	0.7021
FedCVT	-	-	0.7754	0.6626	0.9460	0.6223	0.7985	-	0.7024	-	0.7435
FedHSSL	-	-	0.7955	0.6952	0.9650	0.6520	0.8280	-	0.7984	-	0.8965

used for knowledge transfer. Similarly, when the features of \mathcal{P}_t change, our mechanism consistently outperforms the version without \mathcal{L}_{mi} . This demonstrates that UniTrans enables hospitals to greatly benefit from cross-institution collaboration.

We then evaluated the role of \mathcal{L}_{cl} in scenarios involving more \mathcal{P}_{ds} . As shown in Fig. 14, \mathcal{L}_{cl} effectively eliminates redundant information, enabling the prediction performance of \mathcal{P}_t to improve slightly as the number of \mathcal{P}_{ds} increases. This demonstrates UniTrans’s ability to enhance scalability and maintain efficient knowledge transfer in multi-party collaboration.

VI. CONCLUSION

In this study, we present a unified vertical federated knowledge transfer framework (UniTrans) designed to transfer knowledge from cross-party overlapping samples to each hospital’s local non-overlapping samples in a domain-adaptive manner. UniTrans exhibits robust dual capabilities, excelling in both intra-domain and cross-domain knowledge transfer. Comprehensive experiments conducted on seven medical datasets validate the framework’s effectiveness in enhancing medical prediction performance for non-overlapping, vulnerable patient groups within participating hospitals.

REFERENCES

- [1] B. McMahan, E. Moore, D. Ramage, S. Hampson, and B. A. y Arcas, “Communication-efficient learning of deep networks from decentralized data,” in *Proceedings of the 20th International Conference on Artificial Intelligence and Statistics, AISTATS 2017, 20-22 April 2017, Fort Lauderdale, FL, USA*, ser. Proceedings of Machine Learning Research, vol. 54. PMLR, 2017, pp. 1273–1282. [Online]. Available: <http://proceedings.mlr.press/v54/mcmahan17a.html>
- [2] T. Yang, G. Andrew, H. Eichner, H. Sun, W. Li, N. Kong, D. Ramage, and F. Beaufays, “Applied federated learning: Improving google keyboard query suggestions,” *CoRR*, vol. abs/1812.02903, 2018. [Online]. Available: <http://arxiv.org/abs/1812.02903>
- [3] A. Act, “Health insurance portability and accountability act of 1996,” *Public law*, vol. 104, p. 191, 1996.
- [4] P. Voigt and A. Von dem Bussche, “The eu general data protection regulation (gdpr):” *A Practical Guide, 1st Ed., Cham: Springer International Publishing*, vol. 10, no. 3152676, pp. 10–5555, 2017.
- [5] C. Huang, L. Wang, and X. Han, “Vertical federated knowledge transfer via representation distillation for healthcare collaboration networks,” in *Proceedings of the ACM Web Conference 2023, WWW 2023, Austin, TX, USA, 30 April 2023 - 4 May 2023*. ACM, 2023, pp. 4188–4199.
- [6] S. Che, Z. Kong, H. Peng, L. Sun, A. D. Leow, Y. Chen, and L. He, “Federated multi-view learning for private medical data integration and analysis,” *ACM Trans. Intell. Syst. Technol.*, vol. 13, no. 4, pp. 61:1–61:23, 2022.
- [7] Y. Liu, T. Fan, T. Chen, Q. Xu, and Q. Yang, “FATE: an industrial grade platform for collaborative learning with data protection,” *Journal of Machine Learning Research*, vol. 22, pp. 226:1–226:6, 2021. [Online]. Available: <http://jmlr.org/papers/v22/20-815.html>
- [8] Z. Ren, L. Yang, and K. Chen, “Improving availability of vertical federated learning: Relaxing inference on non-overlapping data,” *ACM Transactions on Intelligent Systems and Technology*, vol. 13, no. 4, pp. 58:1–58:20, 2022. [Online]. Available: <https://doi.org/10.1145/3501817>
- [9] Y. Kang, Y. Liu, and X. Liang, “Fedcv: Semi-supervised vertical federated learning with cross-view training,” *ACM Transactions on Intelligent Systems and Technology*, vol. 13, no. 4, pp. 64:1–64:16, 2022. [Online]. Available: <https://doi.org/10.1145/3510031>
- [10] Y. He, Y. Kang, X. Zhao, J. Luo, L. Fan, Y. Han, and Q. Yang, “A hybrid self-supervised learning framework for vertical federated learning,” *IEEE Transactions on Big Data*, pp. 1–13, 2024.
- [11] Y. Liu, Y. Kang, C. Xing, T. Chen, and Q. Yang, “A secure federated transfer learning framework,” *IEEE Intell. Syst.*, vol. 35, no. 4, pp. 70–82, 2020.
- [12] S. Orouji, M. C. Liu, T. Korem, and M. A. K. Peters, “Domain adaptation in small-scale and heterogeneous biological datasets,” *Science Advances*, vol. 10, no. 51, p. eadp6040, 2024.
- [13] P. Yang, H. Yang, H. Fu, D. Zhou, J. Ye, T. Lappas, and J. He, “Jointly modeling label and feature heterogeneity in medical informatics,” *ACM Trans. Knowl. Discov. Data*, vol. 10, no. 4, pp. 39:1–39:25, 2016.
- [14] J. T. Zhou, I. W. Tsang, S. J. Pan, and M. Tan, “Multi-class heterogeneous domain adaptation,” *J. Mach. Learn. Res.*, vol. 20, pp. 57:1–57:31, 2019.
- [15] M. Ebrahimi, Y. Chai, H. H. Zhang, and H. Chen, “Heterogeneous domain adaptation with adversarial neural representation learning: Experiments on e-commerce and cybersecurity,” *IEEE Trans. Pattern Anal. Mach. Intell.*, vol. 45, no. 2, pp. 1862–1875, 2023.
- [16] Y. Zhi, W. K. Hau, H. Zhang, and Z. Gao, “Vessel contour detection in intracoronary images via bilateral cross-domain adaptation,” *IEEE J. Biomed. Health Informatics*, vol. 27, no. 7, pp. 3314–3325, 2023.
- [17] Y. Tian, C. Wen, M. Shi, M. M. Afzal, H. Huang, M. O. Khan, Y. Luo, Y. Fang, and M. Wang, “Fairdomain: Achieving fairness in cross-domain medical image segmentation and classification,” in *Computer Vision - ECCV 2024 - 18th European Conference, Milan, Italy, September 29-October 4, 2024, Proceedings, Part LXXVI*, ser. Lecture Notes in Computer Science, vol. 15134. Springer, 2024, pp. 251–271.

- [18] W. M. Kouw and M. Loog, "A review of domain adaptation without target labels," *IEEE Trans. Pattern Anal. Mach. Intell.*, vol. 43, no. 3, pp. 766–785, 2021.
- [19] Y. Yu and H. Lin, "Semi-supervised domain adaptation with source label adaptation," in *IEEE/CVF Conference on Computer Vision and Pattern Recognition, CVPR 2023, Vancouver, BC, Canada, June 17-24, 2023*. IEEE, 2023, pp. 24 100–24 109.
- [20] H. He, O. Queen, T. Koker, C. Cuevas, T. Tsiligkaridis, and M. Zitnik, "Domain adaptation for time series under feature and label shifts," in *International Conference on Machine Learning, ICML 2023, 23-29 July 2023, Honolulu, Hawaii, USA*, ser. Proceedings of Machine Learning Research, vol. 202. PMLR, 2023, pp. 12 746–12 774.
- [21] K. Azizzadenesheli, "Importance weight estimation and generalization in domain adaptation under label shift," *IEEE Trans. Pattern Anal. Mach. Intell.*, vol. 44, no. 10, pp. 6578–6584, 2022.
- [22] Y. Zhou, S. Bai, T. Zhou, Y. Zhang, and H. Fu, "Delving into local features for open-set domain adaptation in fundus image analysis," in *Medical Image Computing and Computer Assisted Intervention - MICCAI 2022 - 25th International Conference, Singapore, September 18-22, 2022, Proceedings, Part VII*, ser. Lecture Notes in Computer Science, vol. 13437. Springer, 2022, pp. 682–692.
- [23] J. Zhou, B. Jing, Z. Wang, H. Xin, and H. Tong, "SODA: detecting COVID-19 in chest x-rays with semi-supervised open set domain adaptation," *IEEE ACM Trans. Comput. Biol. Bioinform.*, vol. 19, no. 5, pp. 2605–2612, 2022.
- [24] X. Yu, D. Zhan, L. Liu, H. Lv, L. Xu, and J. Du, "A privacy-preserving cross-domain healthcare wearables recommendation algorithm based on domain-dependent and domain-independent feature fusion," *IEEE J. Biomed. Health Informatics*, vol. 26, no. 5, pp. 1928–1936, 2022.
- [25] D. Kraft, D. Alnæs, and T. Kaufmann, "Domain adapted brain network fusion captures variance related to pubertal brain development and mental health," *Nature Communications*, vol. 14, no. 1, p. 6698, 2023.
- [26] D. Chai, L. Wang, J. Zhang, L. Yang, S. Cai, K. Chen, and Q. Yang, "Practical lossless federated singular vector decomposition over billion-scale data," in *KDD '22: The 28th ACM SIGKDD Conference on Knowledge Discovery and Data Mining, Washington, DC, USA, August 14 - 18, 2022*. ACM, 2022, pp. 46–55. [Online]. Available: <https://doi.org/10.1145/3534678.3539402>
- [27] W. Xu, H. Zhu, Y. Zheng, F. Wang, J. Zhao, Z. Liu, and H. Li, "ELXGB: an efficient and privacy-preserving xgboost for vertical federated learning," *IEEE Trans. Serv. Comput.*, vol. 17, no. 3, pp. 878–892, 2024.
- [28] C. Li, S. Ding, X. Xu, L. Guo, L. Ding, and X. Wu, "Vertical federated density peaks clustering under nonlinear mapping," *IEEE Transactions on Knowledge and Data Engineering*, pp. 1–14, 2024.
- [29] Y. Liu, Y. Kang, T. Zou, Y. Pu, Y. He, X. Ye, Y. Ouyang, Y. Zhang, and Q. Yang, "Vertical federated learning: Concepts, advances, and challenges," *IEEE Trans. Knowl. Data Eng.*, vol. 36, no. 7, pp. 3615–3634, 2024. [Online]. Available: <https://doi.org/10.1109/TKDE.2024.3352628>
- [30] Z. Guan, Y. Li, Z. Pan, Y. Liu, and Z. Xue, "RFDG: reinforcement federated domain generalization," *IEEE Trans. Knowl. Data Eng.*, vol. 36, no. 3, pp. 1285–1298, 2024.
- [31] J. Yuan, X. Ma, D. Chen, F. Wu, L. Lin, and K. Kuang, "Collaborative semantic aggregation and calibration for federated domain generalization," *IEEE Trans. Knowl. Data Eng.*, vol. 35, no. 12, pp. 12 528–12 541, 2023.
- [32] Z. Feng, Y. Wang, J. Li, F. Yang, J. Lou, T. Mi, R. C. Qiu, and Z. Liao, "Robust and communication-efficient federated domain adaptation via random features," *IEEE Trans. Knowl. Data Eng.*, pp. 1–14, 2024.
- [33] Y. Kang, Y. He, J. Luo, T. Fan, Y. Liu, and Q. Yang, "Privacy-preserving federated adversarial domain adaptation over feature groups for interpretability," *IEEE Transactions on Big Data*, 2022.
- [34] Y. Yan, H. Wang, Y. Huang, N. He, L. Zhu, Y. Xu, Y. Li, and Y. Zheng, "Cross-modal vertical federated learning for MRI reconstruction," *IEEE J. Biomed. Health Informatics*, vol. 28, no. 11, pp. 6384–6394, 2024.
- [35] Q. Pang, Y. Yuan, S. Wang, and W. Zheng, "ADI: adversarial dominating inputs in vertical federated learning systems," in *44th IEEE Symposium on Security and Privacy, SP 2023, San Francisco, CA, USA, May 21-25, 2023*. IEEE, 2023.
- [36] S. Kamara, P. Mohassel, M. Raykova, and S. S. Sadeghian, "Scaling private set intersection to billion-element sets," in *Financial Cryptography and Data Security - 18th International Conference, FC 2014, Christ Church, Barbados, March 3-7, 2014, Revised Selected Papers*, ser. Lecture Notes in Computer Science, vol. 8437. Springer, 2014, pp. 195–215. [Online]. Available: https://doi.org/10.1007/978-3-662-45472-5_13
- [37] T. Chen and C. Guestrin, "Xgboost: A scalable tree boosting system," in *Proceedings of the 22nd ACM SIGKDD International Conference on Knowledge Discovery and Data Mining, San Francisco, CA, USA, August 13-17, 2016*. ACM, 2016, pp. 785–794. [Online]. Available: <https://doi.org/10.1145/2939672.2939785>
- [38] K. Simonyan and A. Zisserman, "Very deep convolutional networks for large-scale image recognition," in *3rd International Conference on Learning Representations, ICLR 2015, San Diego, CA, USA, May 7-9, 2015, Conference Track Proceedings*, Y. Bengio and Y. LeCun, Eds., 2015. [Online]. Available: <http://arxiv.org/abs/1409.1556>
- [39] M. Kosinski, D. Stillwell, and T. Graepel, "Private traits and attributes are predictable from digital records of human behavior," *Proceedings of the National Academy of Sciences*, vol. 110, no. 15, pp. 5802–5805, 2013. [Online]. Available: <https://doi.org/10.1073/pnas.1218772110>
- [40] Y. Cheung, J. Jiang, F. Yu, and J. Lou, "Vertical federated principal component analysis and its kernel extension on feature-wise distributed data," *CoRR*, vol. abs/2203.01752, 2022. [Online]. Available: <https://doi.org/10.48550/arXiv.2203.01752>
- [41] Q. Yang, Y. Liu, T. Chen, and Y. Tong, "Federated machine learning: Concept and applications," *ACM Transactions on Intelligent Systems and Technology*, vol. 10, no. 2, pp. 12:1–12:19, 2019. [Online]. Available: <https://doi.org/10.1145/3298981>
- [42] Y. Saad, *Numerical methods for large eigenvalue problems: revised edition*. SIAM, 2011. [Online]. Available: <https://epubs.siam.org/doi/pdf/10.1137/1.9781611970739.bm>
- [43] A. Vaswani, N. Shazeer, N. Parmar, J. Uszkoreit, L. Jones, A. N. Gomez, L. Kaiser, and I. Polosukhin, "Attention is all you need," in *Advances in Neural Information Processing Systems 30: Annual Conference on Neural Information Processing Systems 2017, December 4-9, 2017, Long Beach, CA, USA*, 2017, pp. 5998–6008.
- [44] T. Xu, W. Chen, P. Wang, F. Wang, H. Li, and R. Jin, "Cdtrans: Cross-domain transformer for unsupervised domain adaptation," in *The Tenth International Conference on Learning Representations, ICLR 2022, Virtual Event, April 25-29, 2022*. OpenReview.net, 2022.
- [45] Z. Xie, S. Tu, and L. Xu, "Multilevel attention network with semi-supervised domain adaptation for drug-target prediction," in *Thirty-Eighth AAAI Conference on Artificial Intelligence, AAAI 2024, Thirty-Sixth Conference on Innovative Applications of Artificial Intelligence, IAAI 2024, Fourteenth Symposium on Educational Advances in Artificial Intelligence, EAAI 2024, February 20-27, 2024, Vancouver, Canada*. AAAI Press, 2024, pp. 329–337.
- [46] R. Meng, X. Li, W. Chen, S. Yang, J. Song, X. Wang, L. Zhang, M. Song, D. Xie, and S. Pu, "Attention diversification for domain generalization," in *Computer Vision - ECCV 2022 - 17th European Conference, Tel Aviv, Israel, October 23-27, 2022, Proceedings, Part XXXIV*, ser. Lecture Notes in Computer Science, vol. 13694. Springer, 2022, pp. 322–340.
- [47] K. Zhou, Z. Liu, Y. Qiao, T. Xiang, and C. C. Loy, "Domain generalization: A survey," *IEEE Trans. Pattern Anal. Mach. Intell.*, vol. 45, no. 4, pp. 4396–4415, 2023.
- [48] M. I. Belghazi, A. Baratin, S. Rajeswar, S. Ozair, Y. Bengio, R. D. Hjelm, and A. C. Courville, "Mutual information neural estimation," in *Proceedings of the 35th International Conference on Machine Learning, ICML 2018, Stockholm, Sweden, July 10-15, 2018*, ser. Proceedings of Machine Learning Research, vol. 80. PMLR, 2018, pp. 530–539.
- [49] A. E. Johnson, T. J. Pollard, L. Shen, L.-w. H. Lehman, M. Feng, M. Ghassemi, B. Moody, P. Szolovits, L. Anthony Celi, and R. G. Mark, "Mimic-iii, a freely accessible critical care database," *Scientific data*, vol. 3, no. 1, pp. 1–9, 2016. [Online]. Available: <https://doi.org/10.1038/sdata.2016.35>
- [50] Kaggle, "Cardiovascular disease dataset," <https://www.kaggle.com/datasets/sulianova/cardiovascular-disease-dataset/data>.
- [51] J. N. Weinstein, E. A. Collisson, G. B. Mills, K. R. Shaw, B. A. Ozenberger, K. Ellrott, I. Shmulevich, C. Sander, and J. M. Stuart, "The cancer genome atlas pan-cancer analysis project," *Nature genetics*, vol. 45, no. 10, pp. 1113–1120, 2013. [Online]. Available: <https://doi.org/10.1038/ng.2764>
- [52] Kaggle, "Heart attack risk prediction dataset," <https://www.kaggle.com/datasets/iamsouravbanerjee/heart-attack-prediction-dataset/data>.
- [53] —, "Prediction of sepsis (sepsis)," <https://www.kaggle.com/datasets/salikhussaini49/prediction-of-sepsis/data>.
- [54] —, "Leukemia classification," <https://www.kaggle.com/datasets/andrewmvd/leukemia-classification/data>.
- [55] —, "Chest x-ray images (pneumonia)," <https://www.kaggle.com/datasets/paultimothymooney/chest-xray-pneumonia/data>.

- [56] A. Qayyum, K. Ahmad, M. A. Ahsan, A. I. Al-Fuqaha, and J. Qadir, "Collaborative federated learning for healthcare: Multi-modal COVID-19 diagnosis at the edge," *IEEE Open J. Comput. Soc.*, vol. 3, pp. 172–184, 2022.
- [57] Q. Yang, J. Zhang, W. Hao, G. P. Spell, and L. Carin, "FLOP: federated learning on medical datasets using partial networks," in *KDD '21: The 27th ACM SIGKDD Conference on Knowledge Discovery and Data Mining, Virtual Event, Singapore, August 14–18, 2021*, F. Zhu, B. C. Ooi, and C. Miao, Eds. ACM, 2021, pp. 3845–3853.
- [58] Z. Zhao, F. Zhou, K. Xu, Z. Zeng, C. Guan, and S. K. Zhou, "LE-UDA: label-efficient unsupervised domain adaptation for medical image segmentation," *IEEE Trans. Medical Imaging*, vol. 42, no. 3, pp. 633–646, 2023.
- [59] C. Chen, Q. Dou, H. Chen, J. Qin, and P. Heng, "Unsupervised bidirectional cross-modality adaptation via deeply synergistic image and feature alignment for medical image segmentation," *IEEE Trans. Medical Imaging*, vol. 39, no. 7, pp. 2494–2505, 2020.
- [60] Y. Liu, Y. Kang, C. Xing, T. Chen, and Q. Yang, "A secure federated transfer learning framework," *IEEE Intelligent Systems*, vol. 35, no. 4, pp. 70–82, 2020. [Online]. Available: <https://doi.org/10.1109/MIS.2020.2988525>
- [61] D. P. Kingma and J. Ba, "Adam: A method for stochastic optimization," in *3rd International Conference on Learning Representations, ICLR 2015, San Diego, CA, USA, May 7–9, 2015, Conference Track Proceedings*, Y. Bengio and Y. LeCun, Eds., 2015.
- [62] D. P. Kingma, "Auto-encoding variational bayes," *arXiv preprint arXiv:1312.6114*, 2013.
- [63] I. O. Tolstikhin, O. Bousquet, S. Gelly, and B. Schölkopf, "Wasserstein auto-encoders," in *6th International Conference on Learning Representations, ICLR 2018, Vancouver, BC, Canada, April 30 - May 3, 2018, Conference Track Proceedings*. OpenReview.net, 2018.
- [64] J. Morrill, A. Kormilitzin, A. Nevado-Holgado, S. Swaminathan, S. Howison, and T. Lyons, "The signature-based model for early detection of sepsis from electronic health records in the intensive care unit," in *2019 Computing in Cardiology (CinC)*. IEEE, 2019.
- [65] K. O'Shea and R. Nash, "An introduction to convolutional neural networks," *CoRR*, vol. abs/1511.08458, 2015. [Online]. Available: <http://arxiv.org/abs/1511.08458>
- [66] Y. Freund, R. Schapire, and N. Abe, "A short introduction to boosting," *Journal-Japanese Society For Artificial Intelligence*, vol. 14, no. 771–780, p. 1612, 1999.
- [67] S. Ö. Arik and T. Pfister, "Tabnet: Attentive interpretable tabular learning," in *Thirty-Fifth AAAI Conference on Artificial Intelligence, AAAI 2021, Thirty-Third Conference on Innovative Applications of Artificial Intelligence, IAAI 2021, The Eleventh Symposium on Educational Advances in Artificial Intelligence, EAAI 2021, Virtual Event, February 2–9, 2021*. AAAI Press, 2021, pp. 6679–6687.



Chung-ju Huang is a Ph.D student in Key Laboratory of High Confidence Software Technologies (Peking University), Ministry of Education, Beijing, 100871, China; School of Computer Science, Peking University, Beijing, 100871, China. His interests include federated learning and responsible AI.



Yuanpeng He is a Ph.D student in Key Laboratory of High Confidence Software Technologies (Peking University), Ministry of Education, Beijing, 100871, China; School of Computer Science, Peking University, Beijing, 100871, China. His interests include computer vision and adaptive software engineering.



Xiao Han received the Ph.D. degree in computer science from Pierre and Marie Curie University and the Institut Mines-TELECOM/TELECOM SudParis in 2015. She is currently a Full Professor with the Beihang University, China. Her research interests include social network analysis, fintech, and privacy protection.



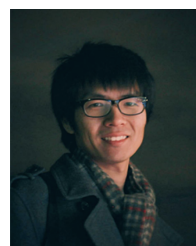
Wenpin Jiao is a professor in the Department of Computer Science and technology, School of EECS, Peking University. He obtained his B.S. and M.S. from East China University of Science and Technology in 1991 and 1997, respectively, and Ph.D. from Institute of Software, Chinese Academy of Sciences in 2000. His research interests include software engineering, adaptive software, multi-agent systems.

Prof. Jiao has published more than 70 research papers, and many of them are published in reputable international journals and conferences, such as *Journal of Software and Systems*, *IET Software*, *Computational Intelligence*, *FSE*, *ICSR*. He is serving as a member of CAAI Knowledge Engineering and Distributed Intelligence Specialized Committee.



Zhi Jin (Fellow, IEEE) received the PhD degree in computer science from Changsha Institute of Technology, China, in 1992. She is currently a professor of computer science at Peking University and the deputy director of Key Lab of High Confidence Software Technologies (Ministry of Education) at Peking University. Her research interests include software engineering, requirements Engineering, knowledge engineering, and machine learning. She has published over 200 scientific articles in refereed international journals, such as *IEEE T-KDE*, *T-SE*, *T-R*, *T-ITS*, *T-PDS*, *ACM T-OSEM*, and *T-CPS*. She has held more than 30 approved invention patents.

She has coauthored five books. She is/was principal investigator of more than 15 national competitive grants. Prof. Jin served/serves as an Associate Editor of *IEEE Transactions on Software Engineering*, *IEEE Transactions on Reliability*, and *ACM Transactions on Autonomous and Adaptive Systems*. She served/serves on the Editorial Board of *Requirements Engineering Journal* and *Empirical Software Engineering*. She is currently a Fellow of the IEEE, Fellow of CCF (China Computer Federation), and the director of CCF Technical Committee of System Software.



Leye Wang is a tenured associate professor at Key Lab of High Confidence Software Technologies (Peking University), MOE, and School of Computer Science, Peking University, China. He received a Ph.D. in computer science from TELECOM Sud-Paris and University Paris 6, France, in 2016. He was a postdoc researcher with Hong Kong University of Science and Technology. His research interests include ubiquitous computing, mobile crowdsensing, and urban computing.

APPENDIX A
PROBLEM FORMULATION

We list the mathematical notions used in this paper in Tbl. VII.

TABLE VII
LIST OF USED NOTIONS.

†Notation	Description
$\mathcal{P}_t, \mathcal{P}_d$	Task hospital and Data hospital.
H_t^{ol}, H_d^{ol}	Overlapping patients between \mathcal{P}_t and \mathcal{P}_d
H_t^{nl}, H_d^{nl}	Non-overlapping patients
X_t, X_d	Feature space of \mathcal{P}_t and \mathcal{P}_d .
I_t, I_d	Patient space of \mathcal{P}_t and \mathcal{P}_d .
Y_t	Labels of \mathcal{P}_t .
H_{fed}^{ol}	Federated latent representations.
Enc	Encoder in LKT module.
\mathcal{L}_{recons}	Reconstruction loss.
\mathcal{L}_{mi}	Mutual information loss.
\mathcal{L}_{cl}	Contrastive loss.

APPENDIX B
EVALUATION SETUP

TABLE VIII
EVALUATION DATASETS.

†Setting	Dataset	Dimension	Class
Intra-domain	MIMIC-III [49]	$58,976 \times 15$	4
	Cardio [50]	$70,000 \times 11$	2
	RNA-Seq [51]	$801 \times 20,531$	5
	Heart [52]	$8,763 \times 26$	2
	Sepsis [53]	$45,852 \times 17$	2
Cross-domain	Leukemia	$12,528 \times 3 \times 128 \times 128$	2
	Pneumonia	$5,863 \times 3 \times 64 \times 64$	2

TABLE IX
DEFAULT DATA PARTITION.

†Dataset	H_t^{nl}	Single Mode		Multiple Mode	
		H_t^{ol}	H_d^{ol}	H_t^{ol}	H_d^{ol}
MIMIC-III	$30,000 \times 5$	$10,000 \times 5$	$10,000 \times 5$	$1,000 \times 5$	$1,000 \times 5$
Cardio	$30,000 \times 5$	$10,000 \times 5$	$10,000 \times 5$	$1,000 \times 5$	$1,000 \times 5$
RNA-Seq	$400 \times 5,000$	$200 \times 5,000$	$200 \times 5,000$	$20 \times 5,000$	$20 \times 5,000$
Heart	3000×9	2000×9	2000×5	200×9	200×5
Sepsis	$30,000 \times 5$	$10,000 \times 5$	$10,000 \times 5$	$1,000 \times 5$	$1,000 \times 5$
Leukemia	$5000 \times$ $3 \times 32 \times 32$	$1000 \times$ $3 \times 128 \times 64$	$1000 \times$ $3 \times 128 \times 64$	$200 \times$ $3 \times 128 \times 64$	$200 \times$ $3 \times 128 \times 64$
Pneumonia	$3000 \times$ $3 \times 24 \times 24$	$1000 \times$ $3 \times 64 \times 32$	$1000 \times$ $3 \times 64 \times 32$	$200 \times$ $3 \times 64 \times 32$	$200 \times$ $3 \times 64 \times 32$

TABLE X
DEFAULT KEY PARAMETERS IN LKT MODULES.

†Backbone	Parameter	Value	Description
AE	depth	3	The depth of encoder and decoder.
	neuron	Sigmoid	The activation function of hidden layers.
VAE	depth	2	The depth of encoder and decoder.
	kld_weight	0.5	The weight of \mathcal{L}_{KL} .
WAE	d_depth	4	The depth of discriminator.
	depth	2	The depth of encoder and decoder.

TABLE XI
DEFAULT KEY PARAMETERS IN TASK-SPECIFIC ML MODELS.

†Model	Parameter	Default
MLP	Hidden layer	$4 \times$ FCNN
	Activation function	ReLU
TabNet	Decision features	32
	Attention features	32
	Decision steps	3
CNN	Hidden layer	$4 \times$ Conv+ $2 \times$ FCNN
	Activation function	Relu
VGG16	Hidden layer	$13 \times$ Conv+ $2 \times$ FCNN
	Activation function	Relu